Crystallization, Melting Behavior, and Wettability of Poly(ε-caprolactone) and Poly(ε-caprolactone)/poly(*N*-vinylpyrrolidone) Blends

Zhimin Xing,[1,2] Guisheng Yang[1,3]

[1]*Beijing National Laboratory for Molecular Sciences, Key Laboratory of Engineering Plastic, Joint Laboratory of Polymer Science and Technology, Institute of Chemistry, Chinese Academy of Sciences, Beijing 100080, China*
[2]*Institute of Chemistry, Graduate School of the Chinese Academy of Sciences, Beijing 100080, China*
[3]*Directorate, Shanghai Genius Advanced Materials Co., Ltd, Shanghai 201109, China*

Received 16 December 2007; accepted 19 January 2009
DOI 10.1002/app.30069
Published online 26 October 2009 in Wiley InterScience (www.interscience.wiley.com).

ABSTRACT: Both wettability and crystallizability control poly(ε-caprolactone)'s (PCL) further applications as biomaterial. The wettability is an important property that is governed by both chemical composition and surface structure. In this study, we prepared the PCL/poly(*N*-vinylpyrrolidone) (PVP) blends via successive *in situ* polymerization steps aiming for improving the wettability and decreasing crystallizability of PCL. The isothermal crystallization of PCL/PVP at different PVP concentrations was carried out. The equilibrium melting point (T_m^0), crystallization rate, and the melting behavior after isothermal crystallization were investigated using differential scanning calorimetry (DSC). The Avrami equation was used to fit the isothermal crystallization. The DSC results showed that PVP had restraining effect on the crystallizability of PCL, and the crystallization rate of PCL decreased clearly with the increase of PVP content in the blends. The X-ray diffraction analysis (WAXD) results agreed with that. Water absorptivity and contact angle tests showed that the hydrophilic properties were improved with the increasing content of PVP in blends. The coefficient for the water diffusion into PCL/PVP blends showed to be non-Fickian in character. © 2009 Wiley Periodicals, Inc. J Appl Polym Sci 115: 2747–2755, 2010

Key words: poly(ε-caprolactone); poly(*N*-vinylpyrrolidone); differential scanning calorimetry; wide-angle X-ray diffraction; water absorptivity; contact angle

INTRODUCTION

Recently, the control of material surface wettability has aroused great interest because of its wide variety of applications in many fields (medicine,[1] catalysis,[2,3] photonics,[3] ultrafiltration,[4] light-emitting diodes,[5] etc.), as attested by the number of articles appeared on this subject. The wettability of materials can be characterized by contact angle (CA). The CA is the angle formed at the intersection of the solid and the fluid interfaces.[6,7] In general, while hydrophobic surfaces show a water CA higher than 90°, in hydrophilic surfaces, the water CA is lower than 90°. The variation of surface wettability can be accomplished by the control of either surface composition and/or surface morphology[8–11] (patterning, roughness, etc.).

Being one of the famous inexpensive biodegradable aliphatic polyesters, PCL is very attractive not only as substitute material for nondegradable polymers for commodity applications but also as a specific plastic in medicine,[12–14] agricultural,[15] drug delivery systems,[16,17] and tissue engineering fields.[18–21] However, its hydrophobic property and semicrystalline nature impart difficulties in developing more advanced biomaterials from PCL,[22,23] because hydrophobic property can lead to slow down degradation kinetics and lacking surface recognition functions for specific mucoadhesion or receptor recognition.[24–26] For improving the desired properties of PCL, many researchers have synthesized PCL copolymers or blends such as PCL/PEG,[27] PCL/polysaccharides,[28–30] PCL/PVC,[31] as well as incorporated various functional groups into PCL.[32,33] Even some PCL-based organic–inorganic hybrid materials have also been synthesized by sol–gel method.[34] Although these investigations are informative, the preparation of functional polyesters usually involves tedious protection/deprotection chemistry and the use of organic solvents. As a result, such systems present significant challenges for their industrial development.

In our previous research,[35] we have prepared PCL/poly(*N*-vinylpyrrolidone) (PVP) blends via successive *in situ* polymerization steps. PVP has good physiological inertia, compatibility, and relatively

Correspondence to: G. Yang (ygs@geniuscn.com).
Contract grant sponsor: 973 Program; contract grant number: 2003CB6156002.

fast hydrolytic degradation.[36,37] PVP can reduce the crystallization rate of many drugs[38–43] as well. In this article, through the comparison of the isothermal crystallization behavior of pure PCL and PCL/PVP blends by differential scanning calorimetry (DSC), we further show that PVP can restrain the crystallinity of PCL. The equilibrium swelling behavior, the penetration rates, and the water diffusion coefficients in pure PCL and PCL/PVP blends are also discussed in this article.

EXPERIMENTAL SECTION

Materials

ε-Caprolactone (CL; Aldrich, Shanghai, China) was dried over CaH_2 for 7 days and distilled at reduced pressure before use. *N*-Vinyl-2-pyrrolidone (NVP; Shanghai Povidone Trade Company, Shanghai, China) was dried under reduced pressure for several hours to remove traces of water before use. Azodiisobutyronitrile (AIBN), ethyleneglycol, and Tin(II) octanoate ($Sn(Oct)_2$) used in this study were all purchased from Shanghai Chemical Reagents Company (Shanghai, China) and used without further treatment.

Polymerization

Freshly vacuum-distilled NVP was dispersed in ε-CL monomer at 80°C with the assigned weight ratio, and then a homogeneous transparent mixture was observed. Then, 0.2 wt % AIBN was added and the mixture was stirred for 24 h at 80°C for the polymerization of NVP. Later, a clear and viscous mixture was obtained. Certain amount of the obtained PVP/CL mixture was kept under vacuum at 100°C for 20 min to remove residual NVP monomer and residual traces of the water. After this, 0.02 wt % ethylene glycol was added and the blend was stirred for 30 min. Then, 0.2 wt % $Sn(Oct)_2$ was added, and the mixture was kept stirred for 24 h at 180°C for the polymerization of ε-CL. The blends obtained were denoted as V10 (PVP 10 wt %) and V20 (PVP 20 wt %).

Measurements

The Waters 991 GPC model was used to evaluate the average molecular weight (M_w) of PCL and PVP and the polydispersity (M_w/M_n) of blends. The molecular weights were calibrated with polystyrene standards. The M_w of the PCL was over 6.0×10^4 g mol^{-1} and the polydispersity (M_w/M_n) was 1.38–1.5. The M_w of the PVP was 1.2×10^4 g mol^{-1} and the polydispersity was 1.4–1.6.

To check the actual NVP content of blends, a nuclear magnetic resonance (NMR) study was carried out. The NMR spectra were obtained with a Bruker Avance DMX500 spectrometer, using $CDCl_3$ as solvent and tetramethylsilane as internal standard.

DSC measurements were carried out on a Perkin-Elmer DSC 7 calibrated by In standards. All the samples were first heated from −50°C to 100°C at a heating rate of 10°C min^{-1} under a nitrogen atmosphere and held at that temperature for 5 min to remove any previous thermal history, and then cooled from 100°C to 0°C at a cooling rate of 10°C min^{-1} under a nitrogen atmosphere. For isothermal crystallization experiments, the samples were heated to 100°C at 200°C min^{-1} and held for 5 min to eliminate small residual nuclei that might act as seed crystals. Then, the melt was cooled rapidly to the crystallization temperature and kept at this temperature for a period of time. After this period, the samples were reheated at 10°C min^{-1} to characterize the melting behavior.

The WAXD measurements were performed at room temperature in a Rigaku D/max 2550 diffractometer operating at a voltage of 40 kV and a current intensity of 100 mA equipped with a curved graphite crystal monochromator and by using the Cu Kα radiation ($\lambda = 0.154056$ nm). The scanning rate was 4°/min, and the scanning range was 5–40° of 2θ. The data were collected at step intervals of 0.02°.

In the water absorptivity test, $20 \times 20 \times 20$ mm^3 samples were first weighed and then immersed into 30 mL deionized water. After keeping the samples in an oven at 37°C for 24 h, they were taken out from deionized water, and then, the water was wiped away from the surface of the samples by using filter paper before they were weighed again. Water absorptivities were determined according to the following equation:

$$\text{Absorptivity} = \frac{W_2 - W_1}{W_1} \times 100\%, \qquad (1)$$

where W_1 and W_2 represent the initial and final weight of the samples. All samples were tested three times in parallel.

Dynamic swelling experiments were performed by placing the dry samples in a distilled water bath at 37.0°C and measuring their weight increase as a time function. The swelling degree W is expressed as the water weight in samples at any instant during swelling.

The CAs on the upper surface of 20×20 mm^2 samples were measured at room temperature with a Dataphysics OCA40 equipment by the sessile drop method, using a 5 μL water droplet in a telescopic goniometer. The telescope had a magnification

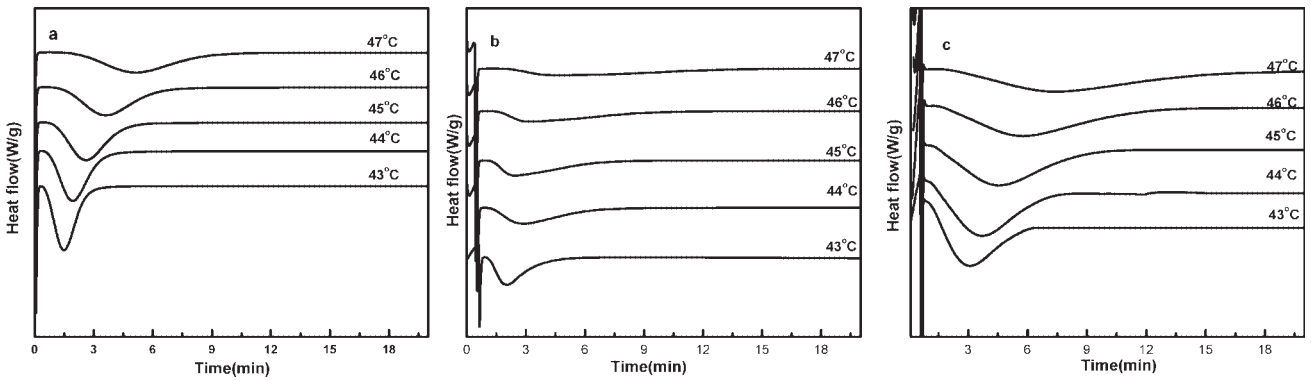

Figure 1 Isothermal crystallization behavior of (a) pure PCL, (b) V10, and (c) V20 at five different crystallization temperatures. The composition is given in the text.

power of 7× and was equipped with a protractor of 0.3° graduation.

RESULTS AND DISCUSSION

Isothermal crystallization kinetics

The PCL and PCL/PVP blends are semicrystalline, which are opaque in appearance. Because the crystallization rate of PCL is very fast, the range of isothermal crystallization temperature for the kinetic study is limited to 43–47°C. Figure 1 shows the exothermic traces for the melt crystallization of pure PCL and PCL/PVP blends with different PVP content at various isothermal crystallization temperatures. It can be seen clearly from Figure 1 that the crystallization exothermic peak shifts to a longer time and becomes flat with increasing crystallization temperature T_c, which implies that the sample with higher crystallization temperature requires a longer time to complete crystallization.

The isothermal crystallization rate is expected to be approximately proportional to the reciprocal of the peak time of endothermic response, t_p, for isothermal crystallization.[44] Figure 2 shows sets of the t_p at different crystallization temperatures for PCL crystallization in blends and homopolymer. In Figure 2, the t_p of sample increases with the isothermal crystallization temperature and the PVP content of blends. Then, the reciprocal of the peak time, representative of the crystallization rate, decreases with the increase of PVP content and isothermal crystallization temperature. Avrami treatment was carried out to examine the crystallization mechanism. According to $\ln(1 - X) = -Kt^n$, where X, K, and n are the fraction of crystallinity at time t, the prefactor, and Avrami index, respectively, crystallization kinetics can be analyzed in terms of the obtained n value. The results of the n values are listed in Table I. The average value of n for the pure PCL crystallization is 2.5, indicating a heterogeneous type of nucleation, in agreement with other studies.[45–47] The averaged value of n in PCL/PVP blends V10 and V20 are 2.7 and 2.8, respectively.

Register and coworkers explored the crystallization of the chemically confined systems.[48,49] They found that the crystallization kinetics within the spherically confined shape exhibits homogeneous nucleation, of which the Avrami index value is 1 and the crystallinity curve appears to be in the first-order crystallization kinetics (i.e., exponential mode).

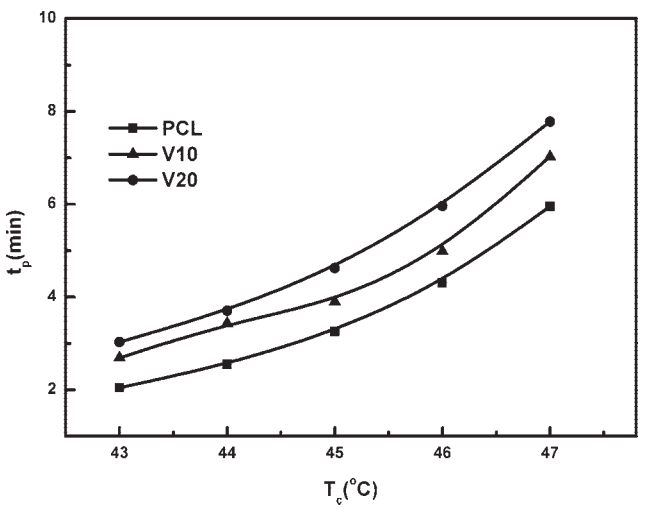

Figure 2 Peak time of endothermic response (t_p) dependence on the crystallization temperature in the isothermal crystallization of PCL, V10, and V20 samples. The composition is given in the text.

TABLE I
Avrami Index of Pure PCL and PCL/PVP Blends

Samples	Avrami exponent n (in average)
PCL	2.5
V10	2.7
V20	2.8

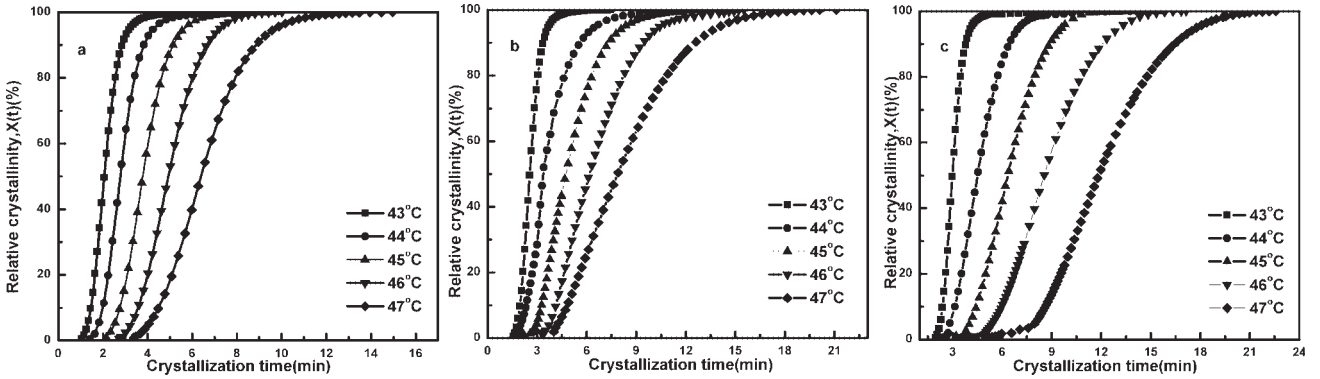

Figure 3 Development of the relative degree of crystallinity $X(t)$ with crystallization times t for the isothermal crystallization of (a) pure PCL, (b) V10, and (c) V20 at five different crystallization temperatures. The composition is given in the text.

By contrast, heterogeneous nucleation shows the traditional sigmoidal kinetics and has an Avrami index value large than 1. Figure 3 shows the crystalline curves of crystallized PCL and PCL/PVP blends; first-order kinetics was not obtained in all the blends. These results suggest that the crystallization of PCL in blends appears as a heterogeneous type of nucleation, and the crystallization kinetics is similar to that of homopolymer. Although the crystallization rate of PCL is affected by the PVP content, the confined size in blends is not small enough to significantly change the crystallization mechanism. Consequently, the heterogeneous nucleation of PCL in PCL/PVP blends is described by an Avrami equation with typical Avrami index below 3.

Melting behavior

The investigation of the melting characteristics is helpful for the determination of the processing parameters of the studied systems. Figure 4 shows the melting behavior of PCL and PCL/PVP blends upon heating at 10°C/min, immediately after being crystallized isothermally at five different temperatures from 43 to 47°C for 30 min. It can be seen that crystallization temperature has a significant effect on the melting behavior of PCL and PCL/PVP blends. With increasing isothermal crystallization temperature, the melting peak temperature moves to higher temperature for all samples. In general, at the same isothermal crystallization condition, the subsequent melting peak temperature, T_m, for PCL is higher than those for PCL/PVP blends. By contrast, significant crystallinity depression was found in samples studied, as shown in Figure 5. The degree of relative crystallinity [$X_r = \Delta H_s/(w_{PCL}\Delta H_p)$] is defined as the ratio of the heat of fusion at the setting temperature (ΔH_s) to the heat of fusion of perfect crystalline PCL in the blends ($w_{PCL}\Delta H_p$), where w_{PCL} is the weight fraction of PCL in the blends. When the isothermal crystallization is performed at 43°C, the difference of T_m between PCL and V10 is more than 1°C, and then

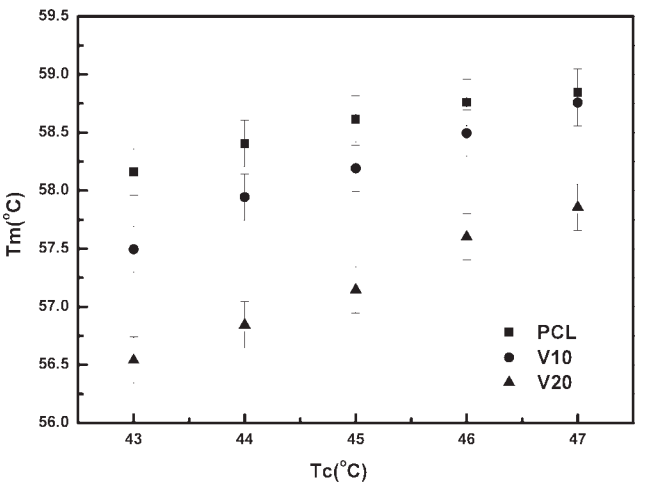

Figure 4 Melting temperature dependence on the crystallization temperature in PCL and in V10 and V20 samples (see text for composition).

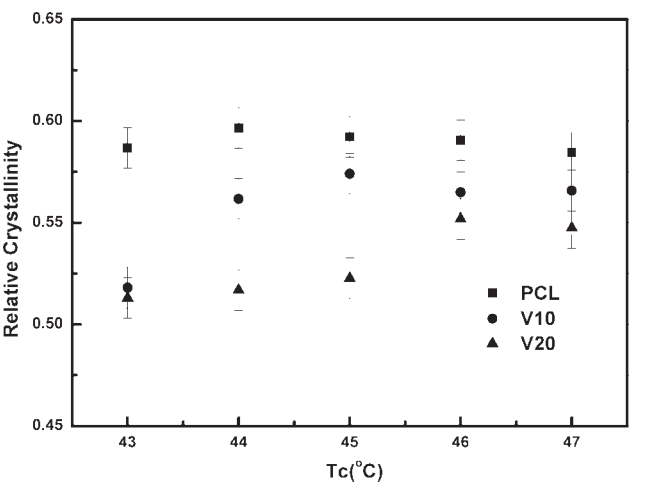

Figure 5 Relative crystallinity dependence on the crystallization temperature in PCL and in V10 and V20 samples (see text for composition).

with the increase of isothermal crystallization temperature, the difference between them becomes smaller. Contrary to the melting of homopolymers, the significant melting depression of PCL crystals can be recognized in blends having the restraining effect for PCL. The restraining effect is related to the content of PVP in blends and crystallization temperature in isothermal crystallization. Because the PVP content of blends V10 is lower than that of V20, the restrained effect of PCL in V10 becomes feebler when the crystallization temperature increases in test range. When the crystallization temperature increased to 47°C, the pure PCL and blends V10 have similar melting points, and at same time, the blends V20 has rather low melting points.

Assessment of equilibrium melting point

The equilibrium melting point (T_m^0) of a homopolymer is the melting point of an infinitely thick crystal based on a specific crystal phase with equilibrium density of internal defects. Crystals of thicknesses in the range of micrometer are made by high-pressure crystallization of a few polymers, e.g., polyethylene.[50] The melting point depression originated by the finite crystal thickness of crystals in the micrometer thickness range is less than 0.1 K, according to calculations based on the Thomson–Gibbs equation. In many cases, the equilibrium melting point is obtained by extrapolation of melting point data (T_m^0) of polymer crystals of finite crystal thickness (L_c). The negligible contribution from the lateral surfaces to the stability of polymer crystals is the basic assumption underlying the Thomson–Gibbs equation:

$$T_m = T_m^0\left[1 - \frac{2\sigma}{\Delta h^0 L_c}\right] \tag{2}$$

where σ is the specific surface free energy of the fold surface and Δh^0 is the heat of fusion at the equilibrium melting point. Extrapolation of T_m–L_c^{-1} data to $L_c^{-1} = 0$ yields the equilibrium melting point provided that the following requirements are fulfilled. (i) The same crystal phase must be present in the crystals of finite thickness as in the infinitely thick, equilibrium crystal. (ii) Crystal rearrangement (e.g., crystal thickening) has to be inhibited during the heating and the recording of the melting point. (iii) Superheating effects must be inhibited. (iv) The specific fold surface free energy must be the same for all samples used for extrapolation. (v) The concentration of defects in the crystals must be the same for all the samples studied and also the same as in the equilibrium crystal. In addition, many polymer samples contain crystals with a distribution in crystal thickness and it is difficult to select a "typical" crystal thickness in a given sample.

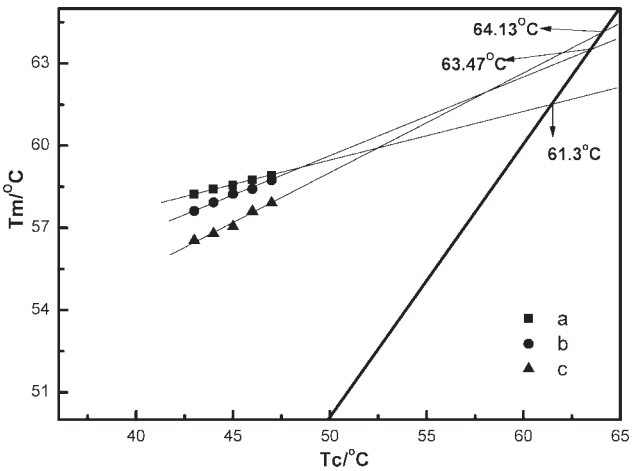

Figure 6 Application of the Hoffman-Weeks approach for determining T_m^0 in (a) PCL and in (b) V10 and (c) V20 samples (see text for composition).

Hoffman and Weeks proposed a method based on the assessment of melting points of crystals grown at different crystallization temperatures (T_c):

$$T_m = \frac{T_c}{\beta} + T_m^0\left[1 - \frac{1}{\beta}\right] \tag{3}$$

where β is the crystal thickening factor $= L_c/L_c^*$; L_c^* being the thickness of the virgin crystal with the melting point equal to the crystallization temperature. Equation (3) is approximately valid provided that the stability of the first formed crystal is just slightly greater than the minimum requirement, i.e., $L_c^* = L_{c,\min} + \delta L_c \approx L_{c,\min}$, where $L_{c,\min}$ is the minimum crystal thickness corresponding to a melting point equal to the crystallization temperature. The equilibrium melting point is according to eq. (3) obtained by extrapolation of $T_m - T_c$ data to $T_m = T_c$; provided β is constant between the different samples used for extrapolation.

Figure 6 clearly reveals that T_m increases linearly with T_c of all samples. The experimental data can be fitted well by the Hoffman and Weeks equation. We determined T_m^0 of PCL and blends according to this approach. The value of β could be obtained from the slope of these fit lines. The values of T_m^0 and β for all samples are summarized in Table II. For pure PCL, we found a T_m^0 of 61.3°C, which is in agreement with the values reported in the literature.[51] After PCL was blended with PVP, T_m^0 substantially increased with increasing content of PVP. In addition, it can also be found from Table II that the β values of the blends are all lower than that of the pure PCL and decrease with increasing the radio of PVP to PCL, indicating that the stability of the PCL crystals in the blends decreases. This effect could be

TABLE II
Equilibrium Melting Temperature T_m^0 and Stability Parameter β for Pure PCL and PCL/PVP Blends

Samples	T_m^0	β
PCL	61.3	5.966
V10	63.5	3.532
V20	64.1	2.776

relative to the confined crystallization of the PCL in the blends.

X-ray diffraction analysis

Figure 7 shows the X-ray diffractograms of PCL and the PCL/PVP blends. Pure PCL shows the peaks at 21.5°, 21.8°, and 23.7° of 2θ, attributed to the (110), (111), and (200) reflections, respectively[52]; although the (200) reflection is actually the overlap of the strong (200) reflection and the much weaker (201), (112), (013), and (104) reflections.[53] In the typical powder X-ray diffraction pattern of PCL/PVP blends, the two strong peaks related to the (110) and (200) reflections and the weak peak related to the (111) reflection are also clearly observed.

It is observed that the position of diffraction peak related to (110) planes in PCL shifted to lower values in the blends with an increasing PVP content. Consequently, the interplanar spacing of (110) planes increased with PVP content, according to the Bragg law. Therefore, it can be concluded that considerable interaction occurs between PCL and PVP in the blends. Moreover, the half width of both peaks was increased, indicating that the crystal size of PCL decreased in the blends with increasing PVP content. This finding is not contradictory with respect to DSC results.

Hydrophilic property

Water absorptivity

Water absorptivity is the simplest test to assess the hydrophilic character of the samples. The dependence of the water absorptivity on the PVP content is shown in Figure 8. Pure PCL is typically hydrophobic with almost 0% water absorptivity, and then with the increase of PVP content of samples, the absorptivity of samples increases linearly with the PVP content until this reaches 25%. When the PVP content increases further, the absorptivity of samples rapidly rises to 105%. The reason is that PVP improves the hydrophilic property of samples, and with the increases of PVP content, the effect is enhanced.

Equilibrium swelling and diffusion

The swelling curves of blends V10 and V20 in water were used for the calculation of a certain diffusion characteristics. As Figure 9 shows, swelling increases initially with time, but, later, constant swelling values are observed. These swelling values can be considered as an equilibrium swelling degree, and they are given in Table III. As shown in Table III, equilibrium-swelling values increase as the PCL content decreases in blends. The hydrophilic capacity of blends increases when the content of PVP in PCL/PVP blends increases. The penetration rate of water for each blends was determined by the method described by Peppas and coworkers[54,55] using eq. (4):

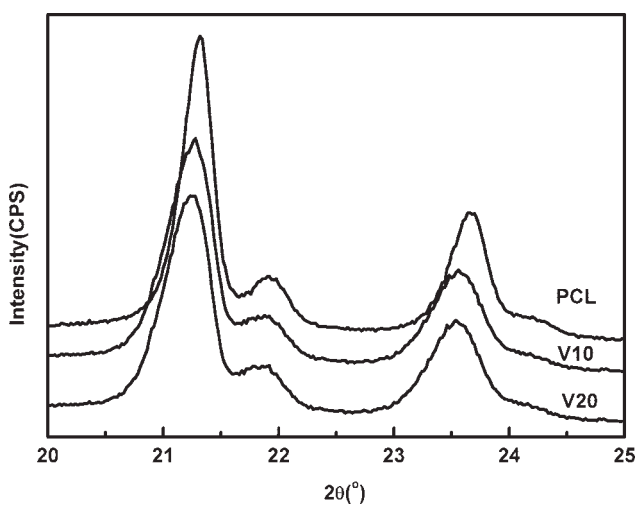

Figure 7 WAXD diagrams for PCL and V10 and V20 blends. The composition is indicated in the text.

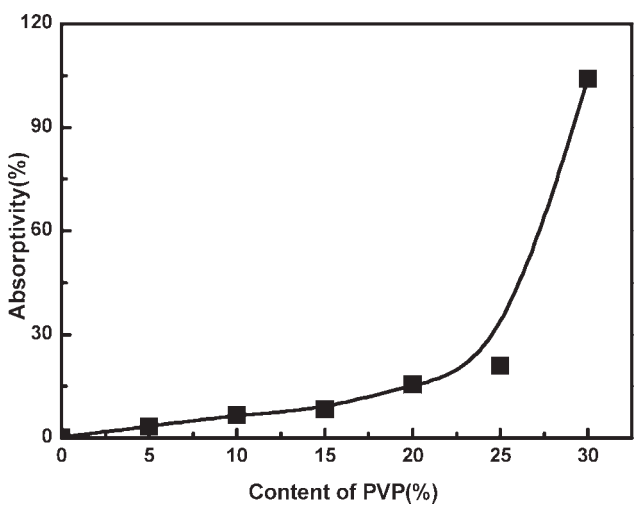

Figure 8 Water absorptivity dependence on the PVP content for PCL and PCL/PVP blends.

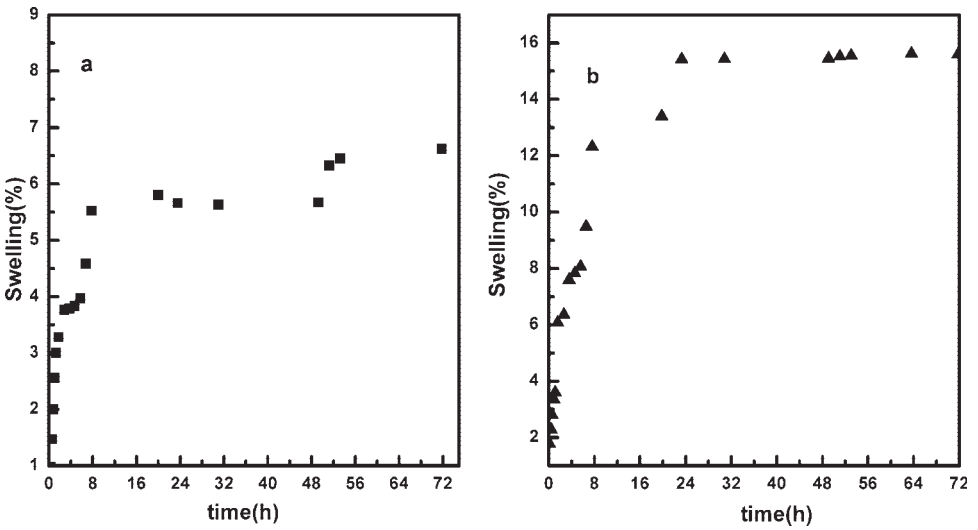

Figure 9 The swelling dependence on time for blends (a) V10 and (b) V20 in water (see text for composition).

$$\nu = \frac{1}{2\rho A}\left(\frac{dW_g}{dt}\right) \quad (4)$$

where ν is the penetration rate; dW_g/dt is the slope of the plot of weight increase versus time; ρ is the density of water at 37°C; and A is the area of one of the faces of the sample. The values obtained are reported in Table III. These results agree with the swelling equilibrium ones. As the PCL concentration increases, more difficult is the water penetration because of the steric impediment created in the blends structure.

Analysis of the mechanisms of water diffusion in polymeric systems has received considerable attention in recent years because of the important applications of swellable polymers in biomedical, pharmaceutical, environmental, and agricultural engineering fields.[56] The following equation was used to determine the nature of water diffusion into PCL/PVP blends[57]:

$$F = M_t/M_\infty = kt^n \quad (5)$$

where M_t and M_∞ denote the amount of solvent diffused into the samples at time t and infinite time (equilibrium), k is a constant related to the structure of the network, and the exponent n is a numerical value that depends on the type of diffusion. For cylindrical shapes, $n \leq 0.50$ and corresponds to Fickian diffusion, whereas $0.50 < n < 1.00$ indicates that diffusion is non-Fickian.[58] Equation (5) was applied to various stages of swelling and plots of ln F against ln t (not shown here) gave straight lines from which the exponents n and k could be calculated. The values are listed in Table IV. It is clearly seen from this table that the values of the diffusion exponent are over 0.50. Thus, it may be assumed that the diffusion of water into PCL/PVP blends is non-Fickian in character.

Contact angle measurement

For further examining the change of hydrophilic property of samples, especially in their surface, CA test was performed. CA measurement is widely used as a simple, sensitive technique for quantifying the hydrophilic/hydrophobic property of a surface.[59] Therefore, aqueous dynamic CA measurements was carried out to investigate the change of CA in the presence of PVP. The CA results are shown in Figure 10. In this figure, PCL shows a hydrophobic character with a water CA of 112°–107°; error was lower than 1.3%. On the opposite, the PCL/PVP blends are hydrophilic, and the CAs decreased dramatically in the first several seconds and retained at the lower angle value for long time. Another

TABLE III
Experimental Data of Equilibrium Swelling and Water Penetration Rate in Samples V10 and V20 at 37°C

Samples	PVP content (NMR)	Equilibrium swelling (%)	ν, penetration rate ($\times 10^{-3}$cm/s)
V10	9.86	6.6	9.42
V20	18.52	15.4	17.28

TABLE IV
Values Obtained for the Constant, k, and the Exponent, n, in the Study of the Water Diffusion in PCL/PVP Blends

Samples	PVP content (NMR)	n	$k \times 10^2$ (h^{-n})
V10	9.86	0.65	33.4
V20	18.52	0.52	39.2

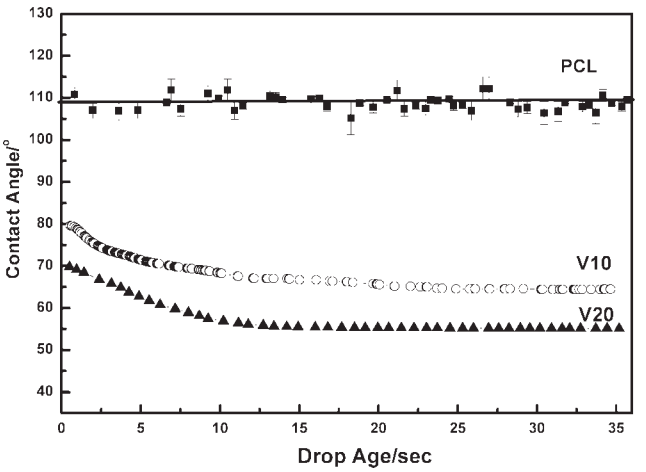

Figure 10 Relationship between the drop age and the water contact angles on the surface of PCL (■), V10 (○), and V20 (▲) samples (see text for composition).

characteristic of blends is confirmed that the final water CA decreases with the increase in the PVP content. Thus, for the V10 system, the final water CA is 63°, and for the V20 system, the final water CA is 55°. It is thus confirmed that PVP has a profound effect on hydrophilic properties of the blends. The surfaces with CAs in the range of 54°–61° have been reported to be optimal for cell adhesion, which is greatly favored by the hydrophilic surfaces with intermediate wettability.[59] These results confirm that PCL/PVP blends, especially the one called V20, may become new biodegradable material for biomedical applications.

CONCLUSIONS

In conclusion, we have presented a facile approach to improve the wettability and to decrease the crystallizability of the PCL by preparing PCL/PVP blends by means of successive *in situ* polymerization steps. The DSC results show that PVP has a restrain effect on the crystallizability of PCL and that this property decreases when the PVP content in the PCL/PVP blends increases. Water absorptivity and CA tests confirm that the hydrophilic properties in PCL/PVP blends are improved when compared with those exhibited by pure PCL. Water diffusion into PCL/PVP blends showed a non-Fickian character. For all these reasons, PCL/PVP blends are considered as promising substitute material for drug delivery, cell therapy, and other biomedical applications.

References

1. Jagielski, J.; Piatkowska, A.; Aubert, P.; Thomé, L.; Turos, A.; Kader, A. A. Surf Coat Technol 2006, 200, 6355.
2. Kamei, M.; Mitsuhashi, T. Surf Sci 2000, 463, L609.
3. Liu, H.; Zhai, J.; Jiang, L. Soft Matter 2006, 2, 811.
4. Asatekin, A.; Kang, S.; Elimelech, M.; Mayes, A. M. J Membr Sci 2007, 298, 136.
5. Chong, L. W.; Lee, Y. L.; Wen, T. C. Thin Solid Films 2007, 515, 2833.
6. Bubert, H.; Ai, X.; Haiber, S.; Heintze, M.; Bröser, V.; Pasch, E.; Brandl, W.; Marginean, G. Spectrochim Acta Part B 2002, 57, 1601.
7. Lam, C. N. C.; Ko, R. H. Y.; Yu, L. M. Y.; Ng, A.; Li, D.; Hair, M. L.; Neumann, A. W. J Colloid Interface Sci 2001, 243, 208.
8. Mizukoshi, T.; Matsumoto, H.; Minagawa, M.; Tanioka, A. J Appl Polym Sci 2007, 103, 3811.
9. Kiss, E.; Takács, M. G.; Bertóti, I.; Butler, E. I. Polym Adv Technol 2003, 14, 839.
10. Gan, D.; Mueller, A.; Wooley, K. L. J Polym Sci Part A: Polym Chem 2003, 41, 3531.
11. Webb, K.; Hlady, V.; Tresco, P. A. J Biomed Mater Res 2000, 49, 362.
12. Woodward, S. C.; Brewer, P. S.; Moatamed, F.; Schindler, A.; Pitt, C. G. J Biomed Mater Res 1985, 19, 437.
13. Pitt, C. G.; Gratzl, M. M.; Kimmel, G. L.; Surles, J.; Sohindler, A. Biomaterials 1981, 2, 215.
14. Kweon, H. Y.; Yoo, M. K.; Park, I. K.; Kim, T. H.; Lee, H. C.; Lee, H. S.; Oh, J. S.; Akaike, T.; Cho, C. S. Biomaterials 2003, 24, 801.
15. Nakayama, A.; Kawasaki, N.; Maeda, Y.; Arvanitoyannis, I.; Ariba, S.; Yamamoto, N. J Appl Polym Sci 1997, 66, 741.
16. Benoit, M. A.; Baras, B.; Gillard, J. Int J Pharm 1999, 184, 73.
17. Coombes, A. G. A.; Rizzi, S. C.; Williamson, M.; Barralet, J. E.; Downes, S.; Wallace, W. A. Biomaterials 2004, 25, 315.
18. Hutmacher, D. W.; Schantz, T.; Zein, I.; Ng, K. W.; Teoh, S. H.; Tan, K. C. J Biomed Mater Res 2001, 55, 203.
19. Waddell, R. L.; Marra, K. G.; Collins, K. L.; Leung, J. T.; Doctor, J. S. Biotechnol Prog 2003, 19, 1767.
20. Verreck, G.; Chun, I.; Li, Y. F.; Kataria, R.; Zhang, Q.; Rosenblatt, J.; Decorte, A.; Heymans, K.; Adriaensen, J.; Bruining, M.; Remoortere, M. V.; Borghys, H.; Meert, T.; Peeters, J.; Brewster, M. E. Biomaterials 2005, 26, 1307.
21. Serrano, M. C.; Pagani, R.; Vallet-Regí, M.; Peňa, J.; Rámila, A.; Izquierdo, I.; Portolés, M. T. Biomaterials 2004, 25, 5603.
22. Zhu, H. G.; Ji, J.; Lin, R. Y.; Gao, C. Y.; Feng, L. X.; Shen, J. C. Biomaterials 2002, 23, 3141.
23. Quirk, R. A.; Chan, W. C.; Davies, M. C.; Tendler, S. J. B.; Shakesheff, K. M. Biomaterials 2001, 22, 865.
24. Gref, R.; Rodrigues, J.; Couvreur, P. Macromolecules 2002, 35, 9861.
25. Rodrigues, J. S.; Santos-Magalhães, N. S.; Coelho, L. C. B. B.; Couvreur, P.; Ponchel, G.; Gref, R. J Controlled Release 2003, 92, 103.
26. Lemarchand, C.; Couvreur, P.; Besnard, M.; Costantini, D.; Gref, R. Pharm Res 2003, 20, 1284.
27. Piao, L. H.; Dai, Z. L.; Deng, M. X.; Chen, X. S.; Jing, X. B. Polymer 2003, 44, 2025.
28. Mano, J. F.; Koniarova, D.; Reis, R. L. J Mater Sci: Mater Med 2003, 14, 127.
29. Huang, L.; Allen, E.; Tonelli, A. E. Polymer 1998, 39, 4857.
30. Shin, K.; Dong, T.; He, Y.; Taguchi, Y.; Oishi, A.; Nishida, H.; Inoue, Y. Macromol Biosci 2004, 4, 1075.
31. Zhang, Y.; Prud'homme, R. E. Macromol Rapid Commun 2006, 27, 1565.
32. Tian, D.; Dubois, P.; Grandfils, C.; Jérôme, R. Macromolecules 1999, 30, 406.
33. Chen, X.; Gross, R. A. Macromolecules 1999, 32, 308.
34. Jiang, S.; Ji, X.; An, L.; Jiang, B. Polymer 2001, 42, 3901.
35. Zhimin, X.; Tingxiu, X.; Guisheng, Y. J Appl Polym Sci 2009, 111, 1676.
36. Lin, W. J. J Biomed Mater Res 1999, 47, 420.
37. Ciardelli, G.; Cristallini, C.; Barbani, N.; Benedetti, G.; Crociani, A.; Travison, L.; Giusti, P. Macromol Chem Phys 2002, 203, 1666.

38. Yoshioka, M.; Hancock, B. C.; Zografi, G. J Pharm Sci 1995, 84, 983.
39. Matsumoto, T.; Zografi, G. Pharm Res 1999, 16, 1722.
40. Crowley, K. J.; Zografi, G. Pharm Res 2003, 20, 1417.
41. Zeng, X. M.; Martin, G. P.; Marriott, C. Int J Pharm 2000, 218, 63.
42. Miyazaki, T.; Yoshioka, S.; Aso, Y.; Kojima, S. J Pharm Sci 2004, 93, 2710.
43. Khougaz, K.; Clas, S. J Pharm Sci 2000, 89, 1325.
44. Cyras, V. P.; Kenny, J. M.; Vázquez, A. Polym Eng Sci 2001, 41, 1523.
45. Goulet, L.; Pudhomme, R. E. J Polym Sci Part B: Polym Phys 1990, 28, 2329.
46. Skoglund, P.; Fransson, A. J Appl Polym Sci 1996, 61, 2455.
47. Balsamo, V.; Calzadilla, N.; Mora, G. A.; Muller, J. J Polym Sci Part B: Polym Phys 2001, 39, 771.
48. Loo, Y. L.; Register, R. A.; Ryan, A. J. Phys Rev Lett 2000, 84, 4120.
49. Loo, Y. L.; Register, R. A.; Ryan, A. J. Macromolecules 2002, 35, 2365.
50. Wunderlich, B. Crystal Nucleation, Growth, Annealing; Academic Press: New York, 1978; Vol. 2: Macromolecular Physics.
51. Nie, K.; Zheng, S.; Lu, F.; Zhu, Q. J Polym Sci Part B: Polym Phys 2005, 43, 2594.
52. Ong, C. J.; Price, F. P. J Polym Sci Part C: Polym Symp 1978, 63, 45.
53. Bittiger, H.; Marchessault, R. H.; Niegisch, W. D. Acta Crystallogr B 1970, 26, 1923.
54. Peppas, N. A.; Franson, N. M. J Polym Sci Polym Phys Ed 1983, 21, 983.
55. Davidson, C. W. R.; Peppas, N. A. J Controlled Release 1986, 3, 259.
56. Buckley, J. D.; Berger, M. J Polym Sci 1962, 56, 163.
57. Crank, J. Mathematics of Diffusion; Oxford University Press: New York, 1970; pp 123–125.
58. Firestone, B. A.; Siegel, R. A. J Appl Polym Sci 1991, 43, 901.
59. Saltzman, W. M. In Principles of Tissue Engineering; Lanza, R. P., Langer, R., Chick, W. L., Eds.; R.G. Landers Company: Georgetown, Texas, 1997; pp 225–246.